

# A new super resolution Bayesian method for pansharpening Landsat ETM+ imagery

Rafael Molina<sup>1</sup>, Javier Mateos<sup>1</sup>, Aggelos K. Katsaggelos<sup>2</sup> and Raul Zurita Milla<sup>3</sup>

<sup>1</sup> Dpto. de Ciencias de la Computación e I.A. Universidad de Granada

<sup>2</sup> Dept. of Electrical Engineering and Computer Science, Northwestern University

<sup>3</sup> Wageningen UR. Centre for Geo-Information

**Abstract:** A new super resolution Bayesian method for pansharpening multispectral images which incorporates sensor characteristics to model the observation process of both the panchromatic and the multispectral images is presented in this paper. The quality of the pansharpened images is assessed both qualitatively and quantitatively. Preliminary results are very promising: the method succeeded in preserving the spectral information while increasing the spatial resolution of the Landsat ETM+ multispectral image. Further research will focus on extending the method to fuse imagery acquired by other sensors.

## 1. Introduction

Pansharpening is a fusion technique used to increase the spatial resolution of a multispectral image by combining it with a high spatial resolution panchromatic (PAN) image. This PAN image is typically acquired from the same platform and simultaneously (or in a very short time span) with the multispectral image.

Several pansharpening methods, some of them using super resolution techniques, have been proposed in the literature (see Molina et al., 2005 for a short review). In this paper, a new super resolution Bayesian method for multispectral images is presented. The method incorporates sensor characteristics to model the observation process of both the panchromatic and the observed multispectral images and also uses prior knowledge to model the expected structure of the high resolution multispectral image that we want to estimate.

Let us assume that the multispectral image,  $y$ , that we would observe under ideal conditions with a high resolution sensor consists of  $B$  bands, each one of size  $p=m \times n$  pixels, is expressed as the column vector formed by the image bands, that is,  $y = [y^{1t}, y^{2t}, \dots, y^{Bt}]^t$  where  $t$  denotes the transpose of a vector or matrix and each band of this multispectral image is written as a column vector by lexicographically ordering its pixels as  $y^b = [y^b(1,1), y^b(1,2), \dots, y^b(m,n)]^t$ ,  $b=1,2,\dots,B$ . In real applications, this image,  $y$ , is not available and, instead, we observe a low resolution multispectral image,  $Y$ , with  $P=M \times N$  pixels,  $M < m$  and  $N < n$ , in each of the  $B$  bands. Using the previously described ordering, we have  $Y = [Y^{1t}, Y^{2t}, \dots, Y^{Bt}]^t$ , where the low resolution observed bands are expressed as the column vectors  $Y^b = [Y^b(1,1), Y^b(1,2), \dots, Y^b(M,N)]^t$ ,  $b=1,2,\dots,B$ . Additionally, we observe the high resolution panchromatic image  $x$ , of size  $p=m \times n$  pixels, which using the lexicographical ordering can be expressed as the column vector  $x=[x(1,1), x(1,2), \dots, x(m,n)]^t$ .

Our aim is to reconstruct the multispectral image  $y$  from its corresponding observed low resolution multispectral image  $Y$  and the high resolution panchromatic image  $x$ .

The proposed method uses a linear combination of the high resolution multispectral bands,  $y^b$ , to reproduce the information contained in the PAN image, that is,

$$x = \sum_b \lambda^b y^b + \rho, \quad (1)$$

where  $\lambda^b \geq 0$  are known quantities that weight the contribution of each high spatial resolution multispectral band to the PAN image and  $\rho$  is the observation noise assumed to be Gaussian with zero mean and variance  $1/\gamma$ .

Each high resolution (also called pansharpened) band is furthermore forced to preserve the spectral fidelity to its corresponding low resolution observed band, mathematically,

$$Y^b = H^b y^b + \eta^b, \quad (2)$$

where the matrix  $H^b$  is an integration and decimation operator specifically designed to reproduce the (measured) low resolution band from the reconstructed high resolution band and  $\eta^b$  is the observation noise assumed to be Gaussian with zero mean and variance  $1/\beta^b$ .

## 2. Bayesian modelling and inference

Prior knowledge about the smoothness of the object luminosity distribution within each band makes it possible to model the distribution of  $y$  by a simultaneous auto-regression, SAR (Alvarez et al., 2004), that is,

$$p(y) = \text{const} \times \prod_b \exp\{-\frac{1}{2} \alpha^b \|C y^b\|^2\}, \quad (3)$$

where  $\text{const}$  is a constant,  $C$  denotes the Laplacian operator, and  $\alpha^b$  is the inverse of the variance of the Gaussian distribution.

Given the degradation model for the PAN image described in Eq. (1), the distribution of the panchromatic image  $x$  given  $y$  is defined by

$$p(x|y) = \text{const} \times \exp\left\{-\frac{1}{2} \gamma \left\|x - \sum_b \lambda^b y^b\right\|^2\right\}. \quad (4)$$

We also need to specify the distribution of the observed multispectral image  $Y$  given  $y$  which, from the degradation model described by Eq. (2), is given by

$$p(Y|y) = \text{const} \times \prod_b \exp\{-\frac{1}{2} \beta^b \|Y^b - H^b y^b\|^2\}. \quad (5)$$

Note that, in this formulation, we are not considering any cross-band degradation.

The Bayesian paradigm dictates that inference about the true  $y$  should be based on  $p(y | Y, x)$  given by

$$p(y | Y, x) \propto p(y)p(Y | y)p(x | y). \quad (6)$$

Maximization of this equation with respect to  $y$  yields the maximum *a posteriori* (MAP) estimate of  $y$ .

In this study, the optimization of Eq. (6) is carried out by a cyclic coordinate-descent optimization procedure (Luenberger, 1984) which, to minimize the global cost function, minimizes the cost function with respect to each band in a cyclic fashion; that is, for each iteration of the algorithm, each  $y^b$  is optimized while keeping the rest of the bands  $y^{\underline{b}} = \{j=1, \dots, B, j \neq b\}$ , fixed. When  $y^b$  has been updated, the next band is computed following the same procedure.

Thus, for fixed  $y^{\underline{b}}$ , by substituting Eqs. (3), (4), and (5) into Eq. (6) and maximizing with respect to  $y^b$  we obtain

$$\hat{y}^b = \operatorname{argmin}_{y^b} \alpha^b \|C y^b\|^2 + \beta^b \|Y^b - H^b y^b\|^2 + \gamma \left\| x - \lambda^b y^b - \sum_{j \in \underline{b}} \lambda^j y^j \right\|^2.$$

Minimization of this equation can be carried out by the following iterative gradient descent algorithm

$$y_{i+1}^b = y_i^b - \varphi \left( \alpha^b C^t C y_i^b - \beta^b H^{b^t} (Y^b - H^b y_i^b) - \gamma \lambda^b \left( x - \lambda^b y_i^b - \sum_{j \in \underline{b}} \lambda^j y^j \right) \right), \quad (9)$$

where  $y_{i+1}^b$  and  $y_i^b$  are the high resolution estimates of the band  $b$  at the  $(i+1)$ -th and  $i$ -st iteration steps, respectively, and  $\varphi$  is the relaxation parameter that controls the convergence of the algorithm.

The process is summarized by the following algorithm:

1. Select an initial value  $y^b$  for each  $b = 1, 2, \dots, B$ .
2. For each band  $b = 1, 2, \dots, B$ 
  - a. Set  $i = 0$ ,  $y_{old}^b = y^b$ , and  $y_0^b = y^b$ .
  - b. Compute  $y_{i+1}^b$  according to Eq. (9).
  - c. If  $|y_{i+1}^b - y_i^b| > \mu$  then  $i = i + 1$  and goto step 2.b.
  - d. Set  $y^b = y_{i+1}^b$ .
3. If  $|y^b - y_{old}^b| > \varepsilon$  for at least one band  $b$ , goto step 2.

### 3. Experiments and results

To illustrate the theoretical analysis developed in the previous section an orthorectified Landsat 7 ETM+ image covering the central part of The Netherlands was selected for this study.

The image was acquired over The Netherlands on May 13, 2000. Orthorectified images are images already corrected from terrain and/or satellite viewing geometry and with accurate geodetic coordinates (see Tucker et al., 2004 for a more detailed review on the characteristics of the Landsat orthorectified dataset). Orthorectified images are delivered with all the spectral bands at their native spatial resolution which is of 14.25m for the PAN image and 28.5 for the multispectral bands. The digital numbers of the image were transformed into

radiance values by applying the gains and offsets that have been published for this sensor.

A subset of 1024 by 1024 pixels of the multispectral image plus its corresponding 2048 by 2048 pixels of the PAN image were selected for high resolution image reconstruction (pansharpening). The central part of the selected subset, centered on 52.453°N, 5.876°E, is depicted in Figure 1.

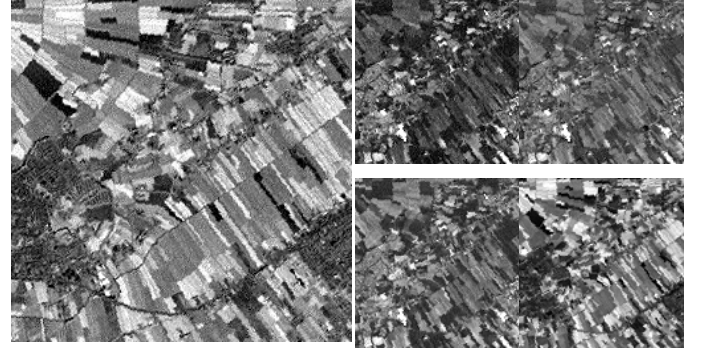


Figure 1. Original Landsat ETM+ image: (left) PAN band. (right) from left to right and top down, the multispectral bands 1 to 4.

Figure 2 depicts the (normalized to one) sensor response for each band of the Landsat 7 ETM+ image. Note that the PAN band covers the spectral region from almost the end of band 1 until the end of band 4, and that the sensor spectral response is not constant over the whole range. The values of  $\lambda^b$  in Eq. (4) were obtained from the spectral response of the ETM+ sensor by summing up the spectral response of the PAN band for each multispectral band range and, subsequently, normalizing them to add to one (Table 1). Notice that  $\lambda^5$  and  $\lambda^7$  are both zero because the bands 5 and 7 do not spectrally overlap with the PAN band.

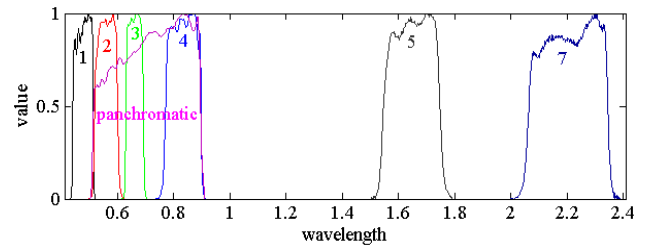


Figure 2. Landsat 7 ETM+ band spectral response.

TABLE I. OBTAINED VALUES FOR  $\lambda^b$

Band	1	2	3	4	5	7
$\lambda^b$	0.015606	0.22924	0.25606	0.49823	0.0	0.0

The parameters of the Bayesian model were experimentally chosen to be  $\alpha^b = 0.01$  and  $\beta^b = 1.0$ , for all the bands, and  $\gamma = 0.3$ . The initial value for each high resolution band  $y^b$ ,  $b = 1, 2, \dots, B$ , in the algorithm step 1 was obtained by cubic interpolation of its corresponding low resolution band  $Y^b$  and the iterative procedure thresholds were selected to be  $\mu = 0.01$  and  $\varepsilon = 0.01$ . The obtained pansharpened image is shown in Figure 3.

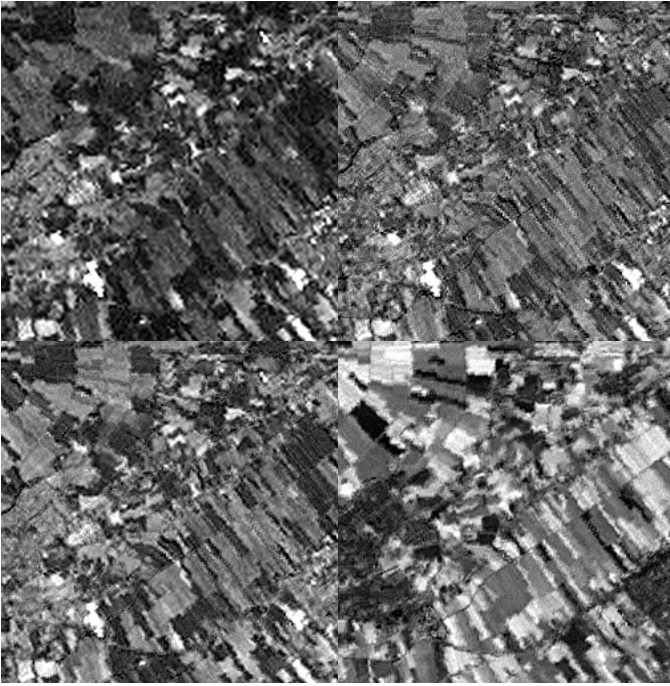


Figure 3. From left to right and top down: Fused image bands 1, 2, 3 and 4.

A qualitative and quantitative analysis of the pansharpened image was performed to assess the spectral and spatial quality of the estimated high resolution image. A visual comparison of the upsampled observed and the pansharpened images indicates that the reconstructed image significantly enhances the spatial content of the observed multispectral image.

For the quantitative analysis, five main quality indices were selected: ERGAS (Wald, 2002), the normalized RMSE (or RMSE<sub>norm</sub>, which equals the spectral RMSE divided by the mean radiance of each band), the mean bias, the coefficient of correlation of the details of the PAN image and the pansharpened image, COR (Tsai, 2004) and, the universal image quality index, UIQI (Wang and Bovik, 2004).

ERGAS is an adimensional index that summarizes the spectral quality of a reconstructed image. In order to compare the pansharpened bands with the observed (multispectral) ones, the pansharpened image was first resampled to 28.5m using a mean filter. An ERGAS value of 1.808 was obtained for this image. This value indicates a good reconstruction because according to Wald (2002) when the ERGAS is below 3.0 then the reconstruction can be considered as a success.

The values for the rest of the indices are summarized in Table II. Notice the low RMSE<sub>norm</sub> values and the very close to zero values of the bias of the mean radiance for each band. The COR values for bands 2, 3, and 4 are relatively high, indicating a successfully incorporation of the PAN details into the pansharpened bands, whereas for band 1 the COR is poor. This poor value can be explained by looking at Table I where it can be observed that band 1 has the lowest contribution to the PAN signal. Therefore the details of this band do not necessarily have to match the ones of the PAN image. Finally, the UIQI values between the resampled to 28.5m pansharpened

bands and the multispectral bands are presented. The UIQI accounts for the loss of correlation and the radiometric and contrast distortions between two images. If both images are identical the UIQI equals to 1. In this case, band 1 presents the best UIQI value while the rest of the bands present a lower but still very good (>0.9) UIQI values.

TABLE II. QUANTITATIVE EVALUATION OF THE FUSED IMAGE

Index	B1	B2	B3	B4
RMSE <sub>norm</sub>	0.0019	0.0316	0.0505	0.0410
Mean bias	-0.0007	-0.0142	-0.0160	-0.0310
COR	0.1163	0.7921	0.7502	0.8152
UIQI	0.9996	0.9489	0.9543	0.9683

#### 4. Conclusions and Outlook

A new super resolution Bayesian method for pansharpening multispectral images has been presented. The performance of this pansharpening method has been assessed both qualitatively and quantitatively. The results are very promising, since the method succeeded in preserving the spectral information (ERGAS=1.808) while increasing the spatial resolution of Landsat 7 ETM+ multispectral bands. Further research will focus on extending the method to pansharpen imagery acquired by other sensors.

#### References

- [1] Alvarez, L.D., Molina, R., and Katsaggelos, A.K. (2004) *High resolution images from a sequence of low resolution observations* in T. R. Reed (Ed.), *Digital Image Sequence Processing, Compression and Analysis* (ch. 9, pp. 233-259), CRC Press.
- [2] Luenberger, D.G. (1984). *Linear and Nonlinear Programming*, Reading, MA: Addison-Wesley
- [3] Molina, R., Mateos, J., and Katsaggelos, A.K. (2005) *Super resolution reconstruction of multispectral images*, Proc. iAstro Workshop on Virtual Observatories, in press.
- [4] Tsai, V.J.D. (2004) *Evaluation of multiresolution image fusion algorithms*. in International Geoscience and Remote Sensing Symposium (IGARSS).
- [5] Tucker, C.J., Grant, D.M., and Dykstra, J.D. (2004) *NASA's global orthorectified Landsat data set*. *Photogrammetric Engineering & Remote Sensing*, 70(3):313-322.
- [6] Wald, L. (2002) *Data fusion, definitions and architectures. Fusion of images of different spatial resolution*. Les Presses de l'Ecole des Mines. Paris (France).
- [7] Wang, Z. and Bovik, A.C. (2002) *A universal image quality index*. *IEEE Signal Processing Letters*, 9(3):81-84.

Address:

R. Molina and J. Mateos. Dpto. de Ciencias de la Computación e I.A. Universidad de Granada.18071 Granada, Spain. ({rms, jmd}@decsai.ugr.es)

A. K. Katsaggelos. Dept. of Electrical Engineering and Computer Science, Northwestern University 2145 Sheridan Rd, Evanston, IL, USA (aggk@ece.northwestern.edu)

R. Zurita Milla. Wageningen UR. Centre for Geo-Information. P.O.Box 47. 6700 AA Wageningen, The Netherlands (raul.zurita-milla@wur.nl)

